IEC/TR 61282-10

Edition 1.0 2013-01

TECHNICAL REPORT

colour inside

Fibre optic communication system design guides – Part 10: Characterization of the quality of optical vector-modulated signals with the error vector magnitude

IEC/TR 61282-10:2013(E)

IEC Central Office
3, rue de Varembé
CH-1211 Geneva 20
Switzerland

Tel.: +41 22 919 02 11
Fax: +41 22 919 03 00
info@iec.ch
www.iec.ch

About the IEC

The International Electrotechnical Commission (IEC) is the leading global organization that prepares and publishes International Standards for all electrical, electronic and related technologies.

About IEC publications

The technical content of IEC publications is kept under constant review by the IEC. Please make sure that you have the latest edition, a corrigenda or an amendment might have been published.

Useful links:

IEC publications search - www.iec.ch/searchpub

The advanced search enables you to find IEC publications by a variety of criteria (reference number, text, technical committee,…).
It also gives information on projects, replaced and withdrawn publications.

IEC Just Published - webstore.iec.ch/justpublished

Stay up to date on all new IEC publications. Just Published details all new publications released. Available on-line and also once a month by email.

Electropedia - www.electropedia.org

The world's leading online dictionary of electronic and electrical terms containing more than 30 000 terms and definitions in English and French, with equivalent terms in additional languages. Also known as the International Electrotechnical Vocabulary (IEV) on-line.

Customer Service Centre - webstore.iec.ch/csc

If you wish to give us your feedback on this publication or need further assistance, please contact the Customer Service Centre: csc@iec.ch.

IEC/TR 61282-10

Edition 1.0 2013-01

TECHNICAL REPORT

colour inside

Fibre optic communication system design guides – Part 10: Characterization of the quality of optical vector-modulated signals with the error vector magnitude

INTERNATIONAL ELECTROTECHNICAL COMMISSION

PRICE CODE V

ICS 33.180.01

ISBN 978-2-83220-567-9

Warning! Make sure that you obtained this publication from an authorized distributor.

CONTENTS

INTERNATIONAL ELECTROTECHNICAL COMMISSION

FIBRE OPTIC COMMUNICATION SYSTEM DESIGN GUIDES –

Part 10: Characterization of the quality of optical vector-modulated signals with the error vector magnitude

FOREWORD

1) The International Electrotechnical Commission (IEC) is a worldwide organization for standardization comprising all national electrotechnical committees (IEC National Committees). The object of IEC is to promote international co-operation on all questions concerning standardization in the electrical and electronic fields. To this end and in addition to other activities, IEC publishes International Standards, Technical Specifications, Technical Reports, Publicly Available Specifications (PAS) and Guides (hereafter referred to as "IEC Publication(s)"). Their preparation is entrusted to technical committees; any IEC National Committee interested in the subject dealt with may participate in this preparatory work. International, governmental and non-governmental organizations liaising with the IEC also participate in this preparation. IEC collaborates closely with the International Organization for Standardization (ISO) in accordance with conditions determined by agreement between the two organizations.
2) The formal decisions or agreements of IEC on technical matters express, as nearly as possible, an international consensus of opinion on the relevant subjects since each technical committee has representation from all interested IEC National Committees.
3) IEC Publications have the form of recommendations for international use and are accepted by IEC National Committees in that sense. While all reasonable efforts are made to ensure that the technical content of IEC Publications is accurate, IEC cannot be held responsible for the way in which they are used or for any misinterpretation by any end user.
4) In order to promote international uniformity, IEC National Committees undertake to apply IEC Publications transparently to the maximum extent possible in their national and regional publications. Any divergence between any IEC Publication and the corresponding national or regional publication shall be clearly indicated in the latter.
5) IEC itself does not provide any attestation of conformity. Independent certification bodies provide conformity assessment services and, in some areas, access to IEC marks of conformity. IEC is not responsible for any services carried out by independent certification bodies.
6) All users should ensure that they have the latest edition of this publication.
7) No liability shall attach to IEC or its directors, employees, servants or agents including individual experts and members of its technical committees and IEC National Committees for any personal injury, property damage or other damage of any nature whatsoever, whether direct or indirect, or for costs (including legal fees) and expenses arising out of the publication, use of, or reliance upon, this IEC Publication or any other IEC Publications.
8) Attention is drawn to the Normative references cited in this publication. Use of the referenced publications is indispensable for the correct application of this publication.
9) Attention is drawn to the possibility that some of the elements of this IEC Publication may be the subject of patent rights. IEC shall not be held responsible for identifying any or all such patent rights.

The main task of IEC technical committees is to prepare International Standards. However, a technical committee may propose the publication of a technical report when it has collected data of a different kind from that which is normally published as an International Standard, for example "state of the art".

IEC 61282-10, which is a technical report, has been prepared by subcommittee 86C: Fibre optic systems and active devices, of IEC technical committee 86: Fibre optics.

The text of this technical report is based on the following documents:

Enquiry draft	Report on voting
86C/1071/DTR	86C/1087/RVC

Full information on the voting for the approval of this technical report can be found in the report on voting indicated in the above table.

This publication has been drafted in accordance with the ISO/IEC Directives, Part 2.

A list of all parts in the IEC 61282 series, published under the general title *Fibre optic system communication system design guides*, can be found on the IEC website.

The committee has decided that the contents of this publication will remain unchanged until the stability date indicated on the IEC web site under "http://webstore.iec.ch" in the data related to the specific publication. At this date, the publication will be

- reconfirmed,
- withdrawn,
- replaced by a revised edition, or
- amended.

A bilingual version of this publication may be issued at a later date.

IMPORTANT – The 'colour inside' logo on the cover page of this publication indicates that it contains colours which are considered to be useful for the correct understanding of its contents. Users should therefore print this document using a colour printer.

0 Introduction

0.1 Introduction to vector modulated signals

Vector or complex modulation is well known since the 1980s in mobile communication and in CATV transmission. In fibre optic telecommunication, coherent transmission was considered during the late 1980s to improve sensitivity and therefore the reach of an optic transmission line. With the introduction of EDFA optical amplification, the need for coherent transmission was then considered less urgent. Recently the foreseeable shortage of transmission capacity and the economic need to optimize transmission capacity without deploying new fibres lead back to the same approach taken for wireless communication in the early 1990s, expanding transmission capacity over a limited number of channels by working with digital complex modulation or vector modulation [1 – 3][1].

The main difference to on-off keying is that vector modulation, as indicated by the name, is characterized by an additional dimension in modulation space:

Modulation:	**on-off**	**vector**
Amplitude	**X**	**X**
Phase	**-**	**X**

0.2 Digital coding with vector modulation

0.2.1 General

The additional phase dimension offers new possibilities for coding a binary signal and in particular for coding more than 1 bit to each digital symbol. That is, a symbol can be assigned to more than the two states 0 and 1. Consider the following bit stream

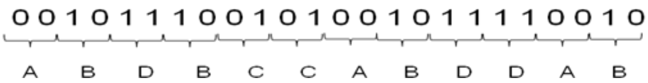

This can, for example, be coded to a symbol alphabet consisting of four elements {A,B,C,D}, as shown. As two bits are combined to a new symbol, only half as many symbols need to be transmitted, reducing the transmission clock by a factor of two. This new reduced clock rate is called symbol rate. Consequently, the symbol rate is half the transmission rate for this case.

In practice, of course, it is not possible to transmit letters, but instead a coding scheme onto the transmitted electromagnetic wave can be selected, such as this:

$$\begin{aligned} 00 &\rightarrow a \times \sin(\omega \times t + 45^\circ) \\ 10 &\rightarrow a \times \sin(\omega \times t + 135^\circ) \\ 11 &\rightarrow a \times \sin(\omega \times t + 225^\circ) \\ 01 &\rightarrow a \times \sin(\omega \times t + 315^\circ) \end{aligned} \tag{1}$$

This example uses a pure phase modulation called quadrature phase-shift keying, QPSK, using four vectors defined by the amplitude of the signal and the four relative phases. If in addition the amplitude is also modulated, it is possible to code more bits to one alphabet of vectors. This is especially the case for higher level QAM signals.

1 Numbers in square brackets refer to the bibliography.

To create these kinds of modulation formats, typically two modulators are needed. These two modulators typically operate respectively in-phase and quadrature, denoted I and Q. This is why this kind of modulator is described as an IQ modulator. The vector signal is described by the two parameters:

$$I = a \times \cos(\phi)$$
$$Q = a \times \sin(\phi) \quad (2)$$

where for the example of QPSK, a signal corresponds to $\varnothing$ values of 45°, 135°, 225° or 315° and the amplitude a is constant.

A common way to display this kind of signal uses IQ or constellation diagrams. In Figure 1, the constellation diagram is shown for the above-described coding scheme.

0.2.2 Constellation diagram

The constellation diagram indicates the amplitude and phase of the signal at the decision point. This is the point in time when the signal must have the correct phase and amplitude value for error-free transmission. This corresponds to the point in on-off modulation where the receiver decides whether the signal is 1 or 0. At each coding location, a cluster of points is displayed, corresponding to a point for each detected symbol in a data pattern.

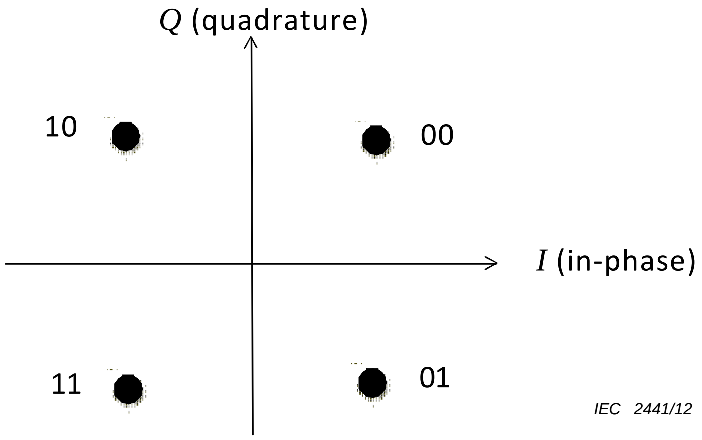

Figure 1 – Constellation diagram for QPSK coding

0.2.3 *IQ* diagram

The IQ diagram displays the complete phase and amplitude transitions between transmitted vectors as the signal is sampled. It reflects directly the combined I and Q components of the signal at any sample time of the data acquisition. The traces on the diagram show the path of the signal vector over the data pattern.

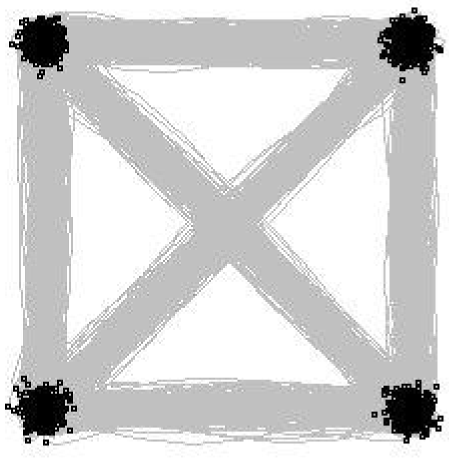

Figure 2 – *IQ* diagram for the same QPSK coding

0.3 Polarization multiplexing

The phase modulation of a signal is demodulated by optical mixing, as described below. The mixing depends on the relative polarization of the two optical carriers. Since the incoming signal generally has an unknown and nonconstant polarization, demodulation then needs to produce demodulated signals for two orthogonal polarization axes. With this doubling of the demodulation information, it is then also possible to detect signals based on two carriers with orthogonal polarization, each carrying independent bit streams, to double the transmission rate for a given wavelength channel. For such polarization multiplexed signals, two independent pairs of I and Q traces exist and two separate constellation or IQ diagrams are used.

0.4 Error vector

Each transmitted symbol is described by a vector with amplitude and phase, which codes a number of bits. Deviations from ideal modulation and impairments during transmission impact the received vector with noise and distortions resulting in a different vector location in the IQ diagram, compared to the reference vector for that symbol, as illustrated in Figure 3.

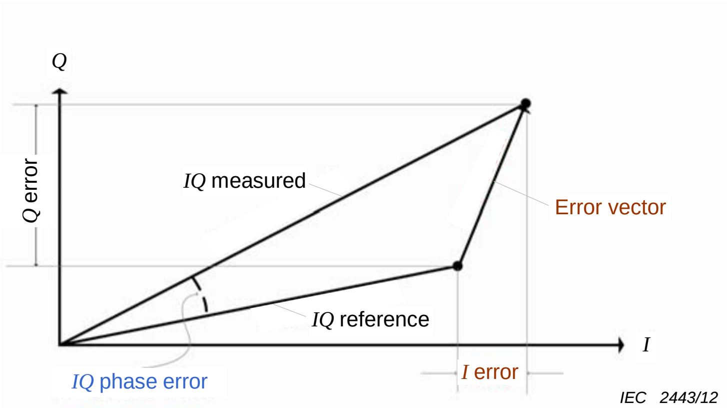

Figure 3 – Relationship of error vector to reference vector and measured signal vector in the constellation diagram

FIBRE OPTIC COMMUNICATION SYSTEM DESIGN GUIDES –

Part 10: Characterization of the quality of optical vector-modulated signals with the error vector magnitude

1 Scope

The purpose of this part of IEC 61282 is to define the error vector magnitude (EVM) as a metric for quantifying the quality of an optical vector-modulated (modulation of phase and possibly magnitude) signal from a transmitter or optical transmission link. The considerations required for reproducible measurement results are detailed. The relationships with other related parameters from constellation diagram analysis like error vector, phase error, magnitude error, I-Q offset and time-resolved EVM are described, as well as the relationship between EVM and Q-factor.

2 Normative references

The following documents, in whole or in part, are normatively referenced in this document and are indispensable for its application. For dated references, only the edition cited applies. For undated references, the latest edition of the referenced document (including any amendments) applies.

IEC 61280-2-8, *Fibre optic communication subsystem test procedures – Digital systems – Part 2-8: Determination of low BER using Q-factor measurements*

3 Terms and definitions

For the purposes of this document, the following terms and definitions apply.

3.1
error vector
difference between a measured IQ vector and the reference vector for the closest symbol D or alternatively for the correct symbol when a known symbol sequence is measured

Note 1 to entry: If the closest symbol and correct symbol differ at the decision point, then the signal is impaired sufficiently to produce a bit error.

3.2
error vector magnitude
EVM
length of a given error vector

Note 1 to entry: For a vector modulated signal that has been measured to give the time-dependent I and Q traces with sampling interval, T_s, as outlined in Clause 5, the EVM of a particular measurement sample with index k is given by

$$\mathrm{EVM}(kT_s) = \sqrt{I_{\mathrm{err}}(kT_s)^2 + Q_{\mathrm{err}}(kT_s)^2} \quad (3)$$

where

$$I_{\mathrm{err}}(kT_s) = \alpha I_{\mathrm{meas}}(kT_s) - I_{\mathrm{ref}}^{\mathrm{r(k)}}$$
$$Q_{\mathrm{err}}(kT_s) = \alpha Q_{\mathrm{meas}}(kT_s) - Q_{\mathrm{ref}}^{\mathrm{r(k)}}$$

and I_{ref} and Q_{ref} correspond to the reference symbol $r(k)$ for the sample k, that is $r(k)$ is an index pointing to the symbol with the reference vector for sample k.

In practical measurements the measured vector has arbitrary magnitude scaling within the receiver sensitivity, so normalization with a factor α of the measured vectors is required to make the error vector independent of the scaling, as described in 4.2.

3.3
RMS error vector magnitude
EVM_{rms}
root-mean-square of the error vector magnitudes for the N symbol decision times of a burst of N symbols, either determined from directly measured samples or interpolated from the neighbouring samples

$$\mathrm{EVM_{rms}} = \sqrt{\frac{1}{N}\sum_{n=1}^{N}\mathrm{EVM}(n)^2} \tag{4}$$

Note 1 to entry: The r.m.s. EVM is usually expressed in per cent of the magnitude of the longest reference vector. In Equation (4), it is assumed that the reference vector and the measured vector are equally scaled with the factor α, as detailed below.

Note 2 to entry: The r.m.s. error vector magnitude of a burst of N measured symbols can be used as a figure of merit for complex signals, specifying the quality of the signal in one number [4].

4 Error vector magnitude calculations and conditions

4.1 Reference vector assignment

The reference vectors are defined as a normalized set of vectors representing the ideal constellation points. Assigning the reference vector for a sample corresponds to determining $r(k)$ in Equation (3). The reference vectors are scaled so that the longest vector has a magnitude of 1. For QPSK or DQPSK the reference vectors are defined as follows:

$$\mathbf{S}_{\mathrm{ref}}^{r} = \begin{pmatrix} I_{\mathrm{ref}}^{r} \\ Q_{\mathrm{ref}}^{r} \end{pmatrix} = \begin{pmatrix} \pm 1/\sqrt{2} \\ \pm 1/\sqrt{2} \end{pmatrix}, \qquad r = 1\ldots 4 \tag{5}$$

In this case, the magnitude of all four symbols is 1. For higher level QAM signals, the values need to be calculated accordingly, such that the outermost symbol has a magnitude of 1.

4.2 Normalization of the measured data

Typically, the measured data have arbitrary scaling; depending on signal strength, link attenuation and receiver responsivity, so it is necessary to normalize the measured data to the reference vectors.

The normalization factor α is chosen to match the measured vectors to the reference by finding the value that minimizes the $\mathrm{EVM_{rms}}$

$$\begin{aligned} &\mathrm{EVM_{rms}} = \sqrt{\frac{1}{N}\sum_{n=1}^{N}\left|\mathbf{S}_{\mathrm{ref}}^{r(n)} - \alpha \times \mathbf{S}_{\mathrm{meas}}(n)\right|^2} \\ &\text{where} \quad \mathbf{S}_{\mathrm{meas}}(n) = \begin{pmatrix} I_{\mathrm{meas}}(n) \\ Q_{\mathrm{meas}}(n) \end{pmatrix} \end{aligned} \tag{6}$$

The r.m.s. error vector magnitude is minimized by solving

$$\frac{\partial \mathrm{EVM_{rms}}}{\partial \alpha} = 0 \tag{7}$$

leading to

$$\alpha = \frac{\sum_{n=1}^{N}\left(I_{\text{ref}}^{r(n)} \times I_{\text{meas}}(n) + Q_{\text{ref}}^{r(n)} \times Q_{\text{meas}}(n)\right)}{\sum_{n=1}^{N}\left(I_{\text{meas}}(n)^2 + Q_{\text{meas}}(n)^2\right)} \tag{8}$$

Note that the same scaling factor is used for both I and Q, so it does not compensate for distortion of the constellation diagram. However, the factor is determined independently for both polarization planes, if the signal is polarization multiplexed. With these values, the normalized detected vector is calculated with the following equations. Here the scaling is shown for each symbol with index n, but it can similarly be applied to all IQ sample pairs with index k.

$$\mathbf{S}_{\text{norm,x}}(n) = \alpha_x \begin{pmatrix} I_{\text{meas,x}}(n) \\ Q_{\text{meas,x}}(n) \end{pmatrix} \qquad \mathbf{S}_{\text{norm,y}}(n) = \alpha_y \begin{pmatrix} I_{\text{meas,y}}(n) \\ Q_{\text{meas,y}}(n) \end{pmatrix} \tag{9}$$

In terms of this normalization, the r.m.s. error vector modulation for the two polarizations is calculated by these equations.

$$\begin{aligned} \text{EVM}_{\text{rms,x}} &= \sqrt{\frac{1}{N}\sum_{n=1}^{N}\left|\mathbf{S}_{\text{ref,x}}^{r(n)} - \mathbf{S}_{\text{norm,x}}(n)\right|^2} \\ \text{EVM}_{\text{rms,y}} &= \sqrt{\frac{1}{N}\sum_{n=1}^{N}\left|\mathbf{S}_{\text{ref,y}}^{r(n)} - \mathbf{S}_{\text{norm,y}}(n)\right|^2} \end{aligned} \tag{10}$$

4.3 Conditions to be specified with EVM_{rms}

The conditions to be specified are as follows:

- measurement bandwidth;
- signal filtering (if used);
- phase tracking bandwidth (if nonlinear tracking is applied).

5 Apparatus for measuring vector modulated signals

5.1 Coherent detector

A set-up to detect and evaluate optical vector modulated signals can be meaningfully described in terms of two main functional parts, a coherent detector and the data postprocessor, as shown in Figure 4.

The coherent detector converts the incoming optical vector modulated signal into an electrical signal which provides its in-phase and quadrature amplitude. Most commonly, the I and Q signals are converted for two orthogonal polarization states, labelled in Figure 4 as x and y. One of the following implementations is usually used: mixing the signal in an optical interferometer with the carrier from a local oscillator or with a delayed fraction of itself.

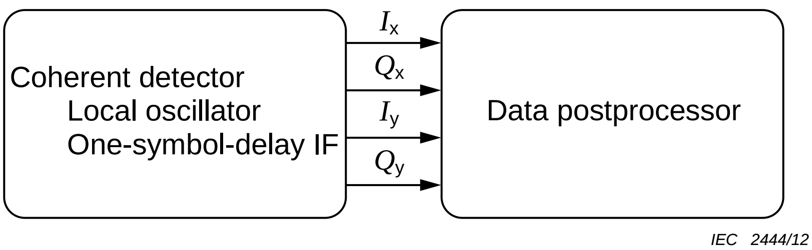

Figure 4 – Block diagram of the main functions for vector signal measurement

5.2 Local oscillator

This implementation uses a coherent light source, i.e. laser, as a local oscillator that is set close to the same frequency as the signal carrier. The frequency offset must be significantly less than the detection bandwidth of the measurement system. Depending on the sampling method, the laser generates either a continuous carrier or short pulses. In each case, the output of the optical detector is digitized and processed to correct for impairments introduced by the optical front end and digitizer.

5.2.1 Detection based on electrical real-time sampling

Figure 5 is a schematic showing the configuration of a coherent detector using a local oscillator for real-time sampling [5].

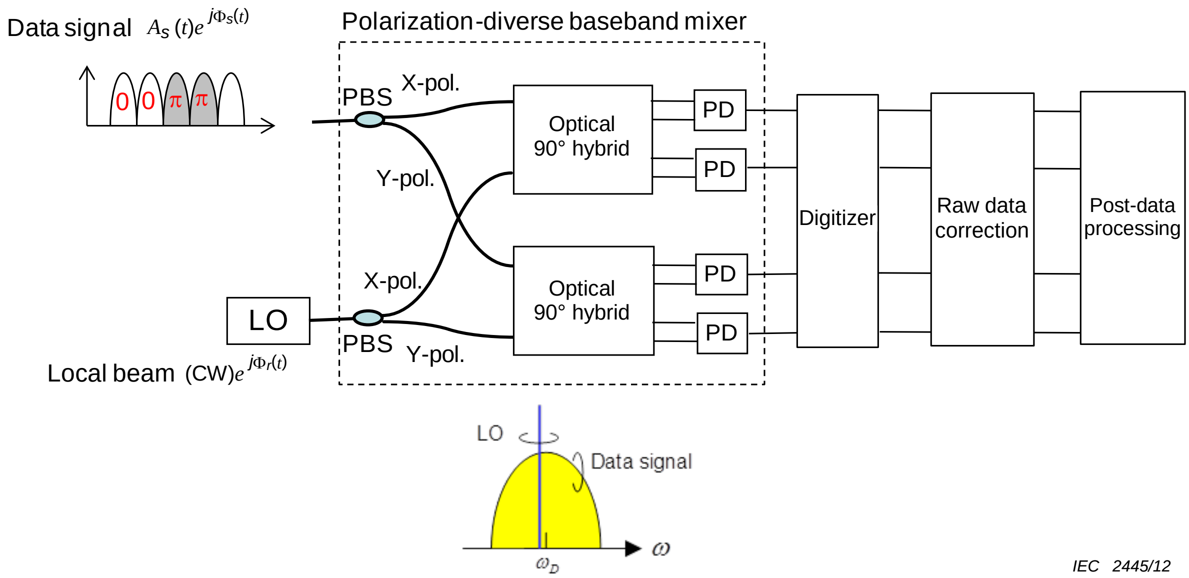

Figure 5 – Configuration based on coherent detection with a local oscillator

For each polarization component, the observed data signal, $A_s(t)e^{j\Phi_s(t)}$, and a continuous local beam, $A_r e^{j\Phi_r(t)}$, are mixed together in an optical 90° hybrid. Here the phases of the signal and reference beams are described by:

$$\Phi_s(t) = \omega_s t + \phi_s(t) + \phi_s + \hat{\phi}_s(t) \tag{11}$$

and

$$\Phi_r(t) = \omega_r t + \phi_r + \hat{\phi}_r(t) \tag{12}$$

where

ω_s and ω_r are the angular frequencies;

$\phi_s(t)$ describes the phase modulation waveform;

ϕ_s describes the initial phase of the signal;

ϕ_r describes the initial phase of the reference;

$\hat{\phi}_s(t)$ and $\hat{\phi}_r(t)$ describe the random variables which show the respective phase noise.

The frequency of the local beam is located at or near the centre of the observed signal bandwidth (homodyne or intradyne detection). The in-phase (I) and quadrature (Q) channels of the optical hybrid are given by:

$$I(t) = \mathrm{Re}\left\{a_1 A_r A_S(t) e^{j\left[\Phi_s(t)-\Phi_r(t)\right]}\right\} \tag{13}$$

and

$$Q(t) = \mathrm{Im}\left\{a_2 A_r A_s(t) e^{j\left[\Phi_s(t)-\Phi_r(t)\right]}\right\} \tag{14}$$

where a_1 and a_2 are the detector gain of the respective detectors.

These analog signals are sampled and converted to digital with the sampling period, T_s. The sampled values are described by

$$I(kT_s) = \mathrm{Re}\left\{a_1 A_r A_S(kT_s) e^{j\left[\Phi_s(kT_s)-\Phi_r(kT_s)\right]}\right\} = 4a_1 A_r A_S(kT_s)\cos\left(\Delta\omega kT_s + \phi_s(kT_s) + \Delta\phi + \hat{\phi}_s(kT_s) - \hat{\phi}_r(kT_s)\right) \tag{15}$$

and

$$Q(kT_s) = Im\left\{a_2 A_r A_s(kT_s) e^{j\left[\Phi_s(kT_s)-\Phi_r(kT_s)\right]}\right\} = 4a_1 A_r A_S(kT_s) sin\left(\Delta\omega kT_s + \phi_s(kT_s) + \Delta\phi + \hat{\phi}_s(kT_s) - \hat{\phi}_r(kT_s)\right) \tag{16}$$

where

$\Delta\omega = \omega_s - \omega_r$ describes the frequency offset;

$\phi_s(kT_s)$ describes the phase modulation to be measured;

$\Delta\phi = \phi_s - \phi_r$ describes the initial phase offset.

The frequency and phase offsets are removed from the I and Q data by the post-processing. For such an offset removing process to work properly, the phase noise

$$\hat{\phi}_s(nT_{symbol}) - \hat{\phi}_r(nT_{symbol}), \tag{17}$$

included in the extracted packet must be sufficiently small. This requires $N_\mathrm{p}T_\mathrm{symbol}$ to be smaller than the laser coherence time. At the same time, for a high-order modulation format in which a large number of constellation elements are used, N_p must be large enough for most elements to appear in the extracted packet. Therefore, a signal light source (laser) is required with a linewidth that is sufficiently narrow for the employed modulation format. Accordingly, in the phase modulation measurement system discussed here, the linewidth of the local oscillator must be as narrow as that of the signal laser.

5.2.2 Detection based on optical equivalent-time sampling

Optical sampling is a technique that measures the time-dependence of optical waves using a gate effect whose response is much faster than that of conventional electronic circuits. Here, we focus on sampling the complex amplitude and exclude techniques that sample only the intensity.

Figure 6 shows the configuration for linear optical sampling (LOS) [6 – 8]. The set-up is similar to that for real-time sampling, but the local beam is a sampling pulse rather than a continuous beam. The interpulse coherence should correspond to a laser linewidth that is compatible with the used sampling rate and phase tracking algorithms. We denote the complex amplitude of the sampling pulse as

$$\delta(t-\tau)e^{j\Phi_r(t)} \tag{18}$$

where

$\delta(t)$ is a function representing the pulse shape;

$\Phi_r(t)$ is the phase of the pulse;

τ is the time of the centre of the pulse.

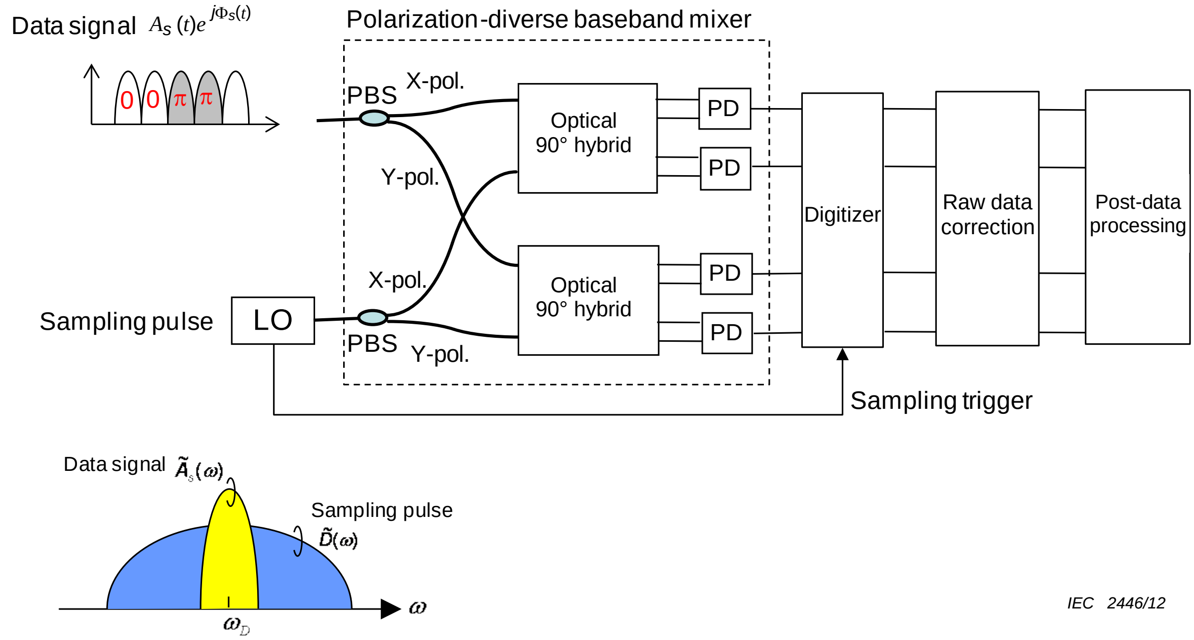

Figure 6 – Configuration for linear optical sampling

Since the electronic circuit that includes the photodetector only responds to the incoming frequency of the sampling pulse train, the photocurrents observed in the I- and Q-channels are integrals during the response time, or the linear correlation of the data and local (pulse) beams. Consequently, we obtain

$$I(\tau) = Re\left\{a_1 \int A_s(t)\delta(t-\tau)e^{j[\Phi_s(t)-\Phi_r(t)]}dt\right\} \tag{19}$$

and

$$Q(\tau) = Im\left\{a_2 \int A_s(t)\delta(t-\tau)e^{j[\Phi_s(t)-\Phi_r(t)]}dt\right\} \tag{20}$$

If the sampling pulse can be approximated by the δ-function, and the detectors' sensitivities, a_1 and a_2 are balanced, we obtain

$$I(\tau) + jQ(\tau) \cong A_s(\tau)e^{j\Phi_s(\tau)}, \tag{21}$$

i.e. the observed signal resembles the instantaneous complex amplitude of the data signal. By scanning the timing of the sampling pulse, τ, with respect to that of the observed data signal, it is possible to reconstruct the entire waveform.

To obtain a meaningful interference signal, the spectrum of the sampling pulse must encompass that of the measured signal. This is shown by using Parseval's equation to transform Equation (21) as:

$$\begin{aligned} I(\tau)+jQ(\tau) &= \int A_S(t)\delta(t-\tau)e^{j\left[\Phi_s(t)-\Phi_r(t-\tau)\right]}dt \\ &= \int \tilde{A}_s(\omega)\tilde{D}^{*}(\omega)e^{j\omega\tau}d\omega \end{aligned} \tag{22}$$

where

$\tilde{A}_s(\omega)$ and $\tilde{D}(\omega)$ are the Fourier transforms of $A_s(t)e^{j\Phi_s(t)}$ and $\delta(t-\tau)e^{j\Phi_r(t-\tau)}$, respectively.

In the spectral domain, we can see that the observed signal is proportional to the product of the spectral amplitudes of the data signal and sampling pulse, and disappears when their overlap is small. Therefore, in typical LOS implementations, the sampling laser must have tunable wavelength to obtain an efficient spectral overlap with the signal. Alternatively, a configuration that uses short optical pulses for a nonlinear-optics gate before making the mixing with a tunable CW LO has also been achieved [8].

Since the optical gate is much faster than the following electronics, very high time-resolution for analyzing temporal waveforms can be achieved, even to the sub-ps level. Hence, an LOS implementation can be designed to have a measurement bandwidth in excess of the signal bandwidth, yielding a distortion-free measurement suitable for e.g. EVM-related analysis in component testing. It should be noted that the equivalent time sampling technique is not specific to optical sampling. It can be used for electrical sampling just as the optical sampling can be implemented as real-time sampling.

A straightforward variation of the procedure for real-time sampling also allows construction of the constellation based on equivalent-time optical sampling [9]. Figure 7 compares the real-time sampling scheme to the equivalent-time sampling scheme. For simplicity here, in both cases the sampling is shown synchronized to the symbol rate, so the samples are at the centre of the symbols. Let T_{os} be the under-sampling period, which is set at MT_{symbol}. M is an integer that shows the ratio of the sampling rate to the symbol rate. As seen in Figure 7, the equivalent-time sampling scheme (b) needs M times the observation time to collect the same number of samples, compared with real-time sampling Figure 7(a) for one sample per symbol. This means that equivalent-time sampling requires M times the coherence of both the data signal and the local (sampling) beam. However, with proper choice of sampling rate it has been shown that equivalent-time optical sampling schemes are compatible with typical laser linewidth used for coherent optical transmission, e.g. for DP-QPSK or DP-16QAM.

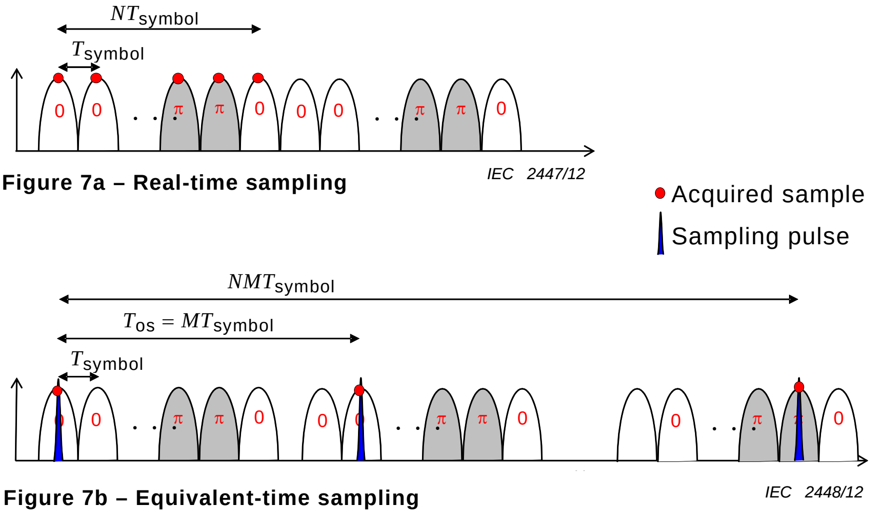

Figure 7a – Real-time sampling

Figure 7b – Equivalent-time sampling

Figure 7 – Schematic comparison of real-time sampling and equivalent-time sampling to observe a repetitive signal pattern

5.2.3 One-symbol delayed interferometer

Differential phase modulation can be detected by using a one-symbol delayed interferometer, without coherent detection [10,11]. A typical set-up is shown in Figure 8. The data signal is divided into two parts, one of which is delayed by the length of one symbol before being introduced into the optical hybrid. Let

$$e^{j\left\{\omega_S t+\phi_S(t)+\hat{\phi}_S(t)\right\}} \tag{23}$$

be the phase-modulated signal, then the output of the I- and Q-channels of the optical hybrid is given by

$$I + jQ = e^{j\left\{-\omega T_{\text{symbol}}+\phi_s(t-T_{\text{symbol}})-\phi_s(t)+\hat{\phi}(t-T_{\text{symbol}})-\hat{\phi}(t)\right\}} \tag{24}$$

These signals are sampled and converted to digital traces. The differential phase is reconstructed by

$$\Delta\phi_{\text{mes}} = \arctan(\frac{Q}{I}) = \phi_s(t-T_{\text{symbol}}) - \phi_s(t) + \hat{\phi}_s(t-T_{\text{symbol}}) - \hat{\phi}_s(t) - \omega_s T_{\text{symbol}} \tag{25}$$

where the last term is the offset to be removed by postprocessing. Equation (25) shows the observed differential modulation, $\varphi_S(t\text{-}T_{\text{symbol}})\text{-}\varphi_S(t)$, and the phase noise contribution, $\hat{\phi}_s(t-T_{\text{symbol}})-\hat{\phi}_s(t)$, which are the same as what is seen in receivers for differential phase modulation formats.

For polarization multiplexed optical signals, the one-bit delay technique requires a polarization tracking device which is set in front of the set-up to separate the X and Y polarization into individual measurement set-ups.

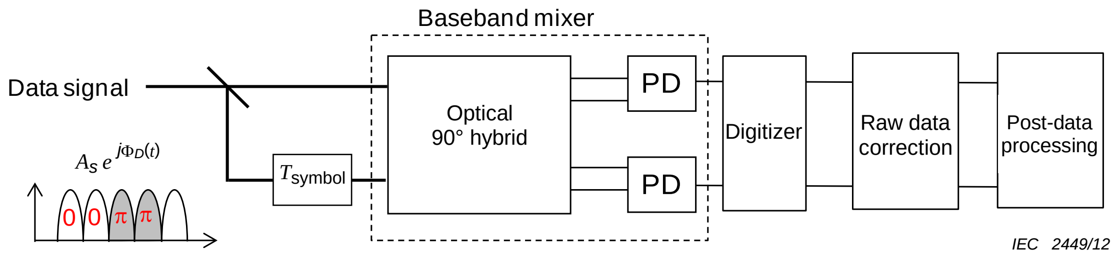

Figure 8 – One-symbol delayed interferometer for detecting differential phase modulation

5.2.4 Constellations of non-differential and differential phase modulation formats

As was described in 5.2.1, the I-Q diagram of (absolute) phase modulation format is described by Equations (13) and (14). The comparable I-Q diagram for differential phase modulation, which is observed in the one-symbol delayed receiver, is described by

$$I_{\text{diff}}(t) = \mathrm{Re}\left\{a_1 A_s\left(t - T_{\text{symbol}}\right)A_s^*(t)e^{j\left\{\phi_s\left(t-T_{\text{symbol}}\right)-\phi_s(t)\right\}}\right\} \tag{26}$$

$$Q_{\text{diff}}(t) = \mathrm{Im}\left\{a_2 A_s\left(t - T_{\text{symbol}}\right)A_s^*(t)e^{j\left\{\phi_s\left(t-T_{\text{symbol}}\right)-\phi_s(t)\right\}}\right\} \tag{27}$$

which can be defined as the differential constellation map in DxPSK formats.

Figure 9 shows a simulation of a QPSK signal measured with a local oscillator reference (left) and with the one-symbol delay interferometer (right). The two IQ diagrams are fundamentally different since the constellation diagram (left) directly represents the amplitude and phase of the optical signal, while the differential constellation diagram (right) displays the phase difference of the optical signal when mixed with itself with a one-symbol relative delay. In addition, the amplitude shown in the differential constellation diagram represents the mixing of the two copies of the signal. Some statistical values, such as the EVM, magnitude error, and phase error, can also be defined for differential phase modulation formats, by using $I_{\text{diff}}(t)$ and $Q_{\text{diff}}(t)$ as in Equations (26) and (27). However, comparing the statistical measures based on absolute phase with the measures based on differential phase is not straightforward. Figure 10 shows an example of a QPSK signal which is distorted by 10° of IQ quadrature error. The distortion affects the constellation diagram differently compared to the differential constellation diagram, which clearly illustrates the difference expected in e.g. a calculated EVM. In the differential phase modulation format, the quality of the signal or the bit error rate is more concerned with the phase error, rather than EVM.

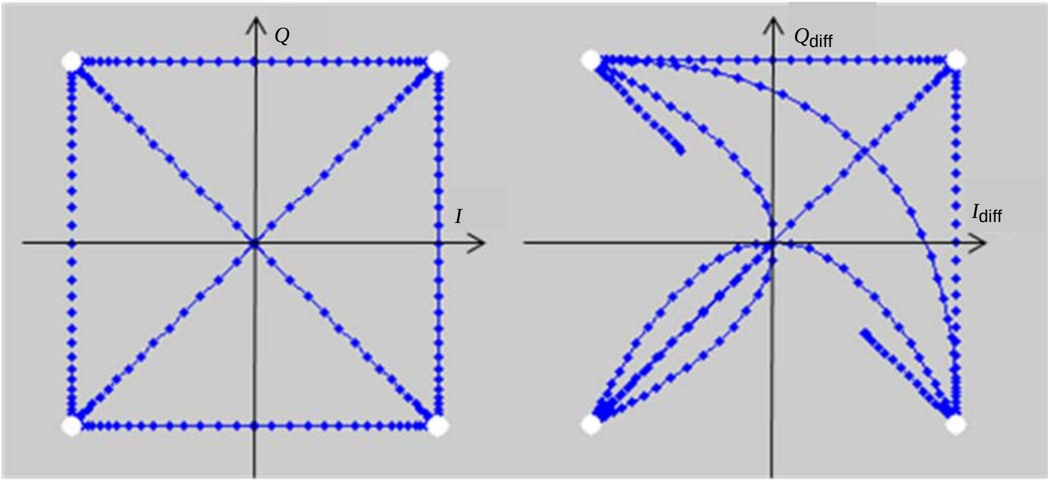

Figure 9 – Simulation of an ideal (D)QPSK signal, represented as a constellation diagram displaying the absolute phase and amplitude of the optical field (left)

With the one symbol delay interferometer technique, the corresponding differential constellation diagram displays the phase difference between two consecutive symbols.

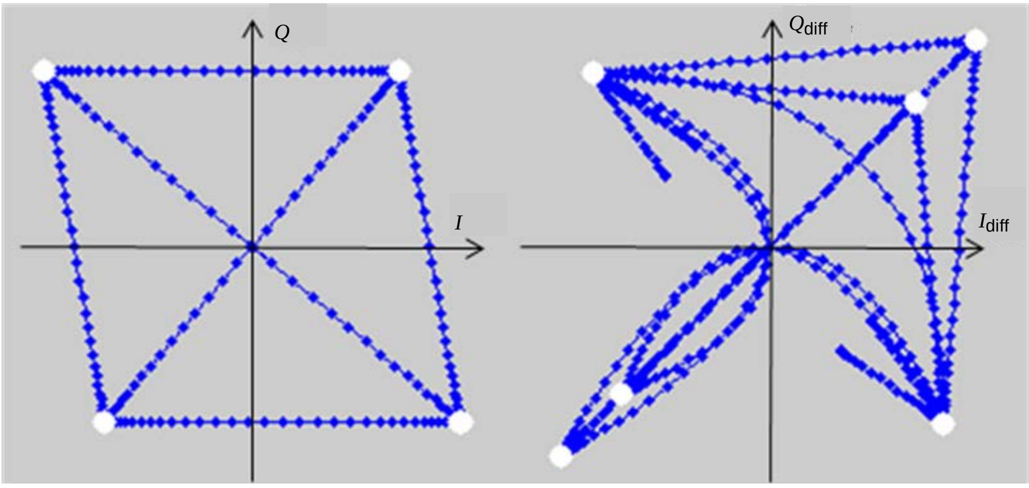

Figure 10 – Simulation of a (D)QPSK signal distorted with 10° *IQ*-quadrature error

Note that the distortion affects the constellation diagram (left) differently than the differential constellation diagram (right). This effect will make EVM comparisons between the two approaches difficult.

5.3 Digital postprocessing

5.3.1 Impairment compensation

The following parameters shall be corrected along the specified wavelength range of a receiver to define the receiver as reference receiver:

- relative timing skew between the signal input S and the I_x, Q_x, I_y, Q_y output;
- phase angle deviation from 90° between I_x and Q_x and between I_y and Q_y;
- offset and relative gain;
- alignment between incoming signal polarization and receiver axes.

A recent overview of digital signal processing for receivers is given in [12].

5.3.2 Relative timing skew

Relative timing skew describes the difference in delay between the optical signal at the input S of the receiver and the output of each digitizer channel with reference to one channel, typically I_x.

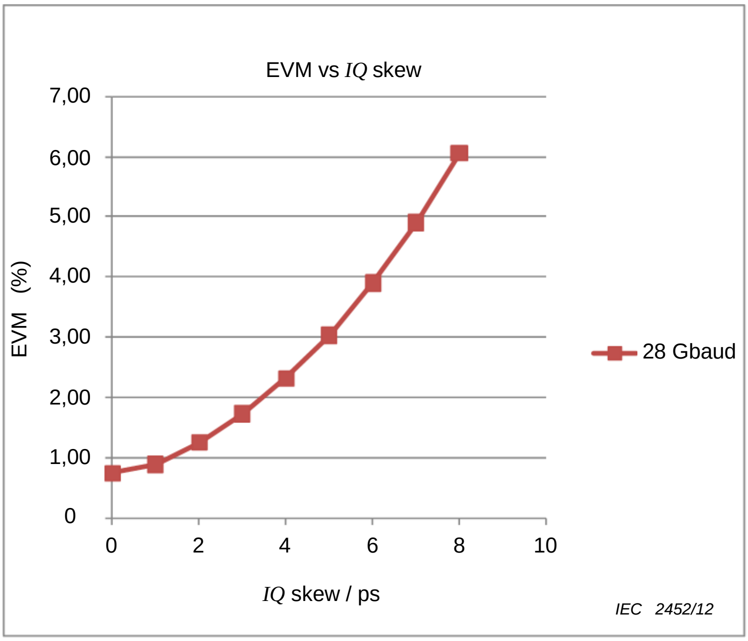

Figure 11 – Calculated influence of impairment

Skew introduces distortion in the constellation position of detected signals and therefore increases EVM.

5.3.3 *IQ* phase angle distortion

For an ideal coherent detector the phase of the in-phase and the quadrature signal is exactly 90°. Generally, however, this phase angle deviates somewhat from 90° and is also wavelength dependent. Figure 12 illustrates this distortion type for a single wavelength.

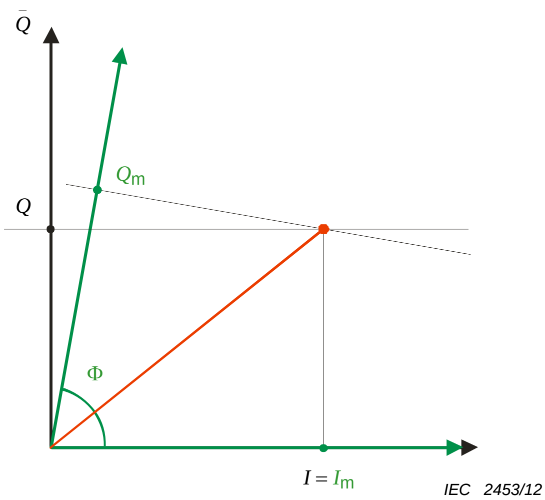

Figure 12 – Error in *I* and *Q* determination from phase angle deviation

The actual measured data are related to the original signal by the following equations, noting that the angle ϕ might depend on the wavelength.

$$\begin{bmatrix} I \\ Q \end{bmatrix} = \begin{bmatrix} 1 & 0 \\ -\cot(\phi) & 1/\sin(\phi) \end{bmatrix} \times \begin{bmatrix} I_m \\ Q_m \end{bmatrix} \tag{28}$$

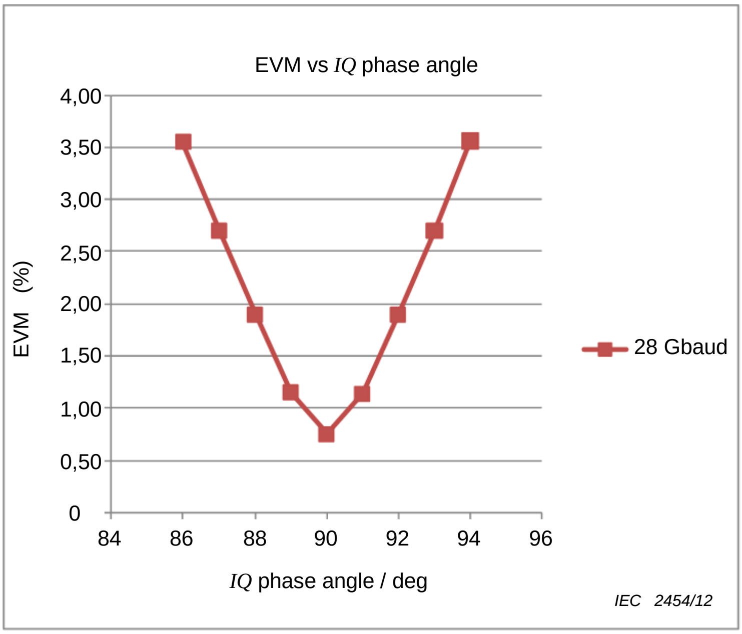

Figure 13 – Calculated influence of impairment

Any deviation in the phase angle between I and Q from 90° leads to distortion of the signal.

5.3.4 Offset and relative gain distortion

In the opto-electrical path of the detector with numerous components, the signal will not be processed with exactly the same gain in each path. In addition, the electrical components incorporate electrical offset to the signal, which will be reflected in the digitized raw data. The difference in the gain of these four paths must be corrected in the raw data together with the offsets incorporated by the electrical components.

In order to correct the data one needs to either measure the unwanted DC offset with an independent measurement or one could simply assume that the baseband signal does not contain any DC part and subtract the DC component found in the measured signal.

In order to correct the gain mismatch between the channels one has again to measure the gain in an independent (calibration) measurement. This gain correction assumes that the variations in gain within the detection bandwidth can be neglected. If this is not true then a de-embedding of the response function of the detector should be applied.

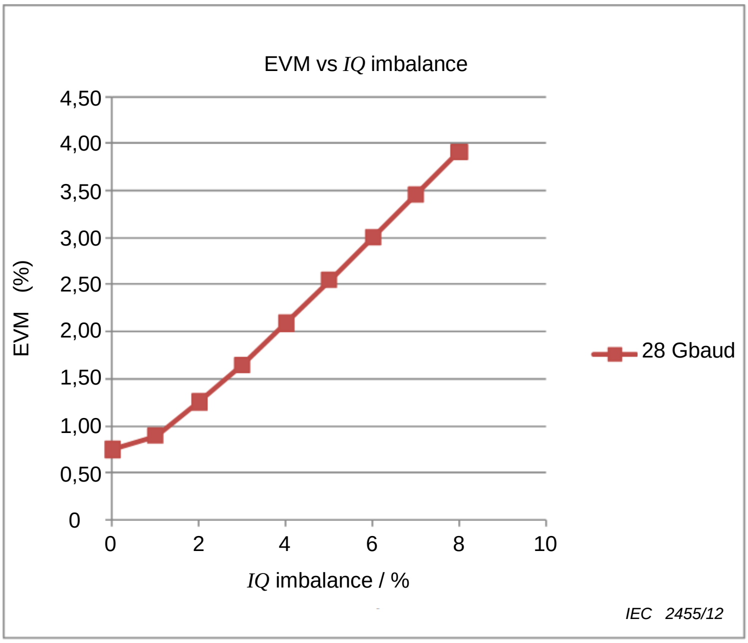

Figure 14 – Calculated influence of impairment

IQ imbalance describes gain ratio between the *I* and *Q* paths of a coherent receiver from signal input to digitizer.

5.3.5 Polarization alignment

In general, the polarization axes of the incoming signal will not be aligned with the coherent detector, so that the signal from the data streams is mixed between the *x* and *y* outputs. This is also the case for a signal that is not multiplexed on both polarization axes. The signals from the four outputs must thus be transformed so that the I_x, Q_x, I_y and Q_y correspond to the original data from the transmitter. This transformation should be performed without improving or impairing the signal quality. If filtering in this step reduces the noise level, then an appropriate correction should be applied to the final EVM_{rms} results.

5.3.6 Corrected results

After applying the corrections described in 5.3.2 to 5.2.5, the signal is described with four data traces $I_x(kT_s)$, $Q_x(kT_s)$, $I_y(kT_s)$, $Q_y(kT_s)$ with k describing the index of the equidistant time samples with an identical time reference. These data traces represent the signal in the way it would have been detected by an ideal detector.

5.3.7 Phase tracking (intradyne detection)

5.3.7.1 Real-time sampling

The coherent detector data represent an optical baseband signal that is usually not completely mixed to zero-frequency offset. This is because perfect wavelength locking between the carrier laser and the local oscillator is not economically possible or necessary. This causes a continuously rising phase (or rotation of the constellation diagram) of the reference receiver output signal, representing the progression of phase difference between the carrier laser and local oscillator laser. This linear phase slope is removed by the tracking to fix the constellation points.

While additional nonlinear phase tracking can also be used to improve demodulation of a signal, this can also remove phase noise and drift that are part of the signal and thus are not recommended for characterizing the transmitted signal quality. If used, this should be noted and described in the results. Such nonlinear tracking can also be used to remove the influence of phase noise in the local oscillator. When this is used, care must be taken to avoid removal of the signal phase-noise influence on the EVM.

Synchronization with the symbol rate is accomplished by subsequent digital processing. Consequently, we can detect the phase at the centre of each symbol

$$\phi_{\text{meas}}(nT_{\text{symbol}}) = \arctan\left(\frac{Q(nT_{\text{symbol}})}{I(nT_{\text{symbol}})}\right) = \Phi_s(nT_{\text{symbol}}) - \Phi_r(nT_{\text{symbol}}) \tag{29}$$

where T_{symbol} is the symbol interval and n is an integer. Substituting Equations (11) and (12) into Equation (29), we obtain

$$\begin{aligned}\phi_{\text{mes}}(nT_{\text{symbol}}) &= \Phi_s(nT_{\text{symbol}}) - \Phi_r(nT_{\text{symbol}}) \\ &= \phi_s(nT_{\text{symbol}}) + \hat{\phi}_s(nT_{\text{symbol}}) - \hat{\phi}_r(nT_{\text{symbol}}) + \Delta\omega nT_S + \Delta\phi,\end{aligned} \tag{30}$$

where the first term $\phi_s(nT_{\text{symbol}})$ on the right hand side shows the phase modulation to be observed. The terms $\hat{\phi}_s(nT_{\text{symbol}}) - \hat{\phi}_r(nT_{\text{symbol}})$ show the random fluctuation of the phase noise of the lasers. $\Delta\omega nT_{\text{symbol}}$ and $\Delta\phi$ are the frequency and phase offsets, respectively.

5.3.7.2 Equivalent time sampling

The discussion on the phase tracking in optical sampling is similar to that for the real-time sampling. The difference in the two schemes is that the data is sampled only with a sampling pulse interval, T_{os}, in the optical equivalent-time sampling, whereas the real-time sampling rate should be two times the signal bandwidth (Nyquist criterion), which for the 28 GBd QPSK example means using about 42 GS/s sampling if a 75 % bandwidth of 21 GHz is used. This elongation of the sampling interval requires more strict tolerance for the frequency offset between the measured signal and sampling pulse, and/or their higher coherence, of the optical sampling. Since in the case of under-sampling with high time resolution there can be many samples during an individual symbol, samples falling into a certain percent of the bit slot corresponding to the decision time can be used to compute the RMS EVM.

5.3.7.3 Delayed interferometer

When observing differential phase shift keying with the one-symbol delayed interferometer, the drift of the signal frequency yield a static rotation of the constellation diagram, as in shown in the term, ωT_{sample}, in Equation (24). This drift can be removed by signal processing to keep the constellation angle to be correct. This process almost covers the demodulation of the signal.

5.3.8 Demodulation (optional)

5.3.8.1 Real-time sampling

In the demodulation of the signal, after subtracting the linear phase slope and assigning the correct absolute phase, the amplitude and phase of the signal is sampled at the symbol clock rate with the correct clock phase. This results in four vectors, I_{x}^{d}, Q_{x}^{d}, I_{y}^{d}, and Q_{y}^{d}, consisting of the detected (d) amplitude and phase values of the symbols. These data are then scaled to fit the normalized magnitudes of the reference constellation for the modulation format. In the final step, evaluation of the shortest Euclidian distance to all possible positions in the constellation diagram determines which symbol was sent. Based on the constellation map the original data stream is recovered.

5.3.8.2 Equivalent time sampling

The demodulation process of PSK and QAM signal in the optical sampling is similar to that in the coherent detection, with the exception that the signal is not resampled at the centre of the symbol slots. Instead, samples measured close to the centre of the symbol slots are used for EVM_{rms} evaluation.

6 Additional measurement parameters to characterize special details of the signal

6.1 Time-resolved EVM

Using the general definition of the EVM each measured sample of the signal under test can be associated with an EVM value. Furthermore, each measured sample can be time stamped and given an accurate measurement time relative to the symbol slot. By combining the time information with the EVM information about each sample, we can define the time-resolved EVM as

$$\mathrm{EVM}(i,t) = \sqrt{I_{\mathrm{err}}(i,t)^2 + Q_{\mathrm{err}}(i,t)^2} \tag{31}$$

where

$$\begin{aligned} I_{\mathrm{err}}(i,t) &= I_{\mathrm{meas}}(i,t) - I_{\mathrm{ref}}^{\mathrm{r(i)}} \\ Q_{\mathrm{err}}(i,t) &= Q_{\mathrm{meas}}(i,t) - Q_{\mathrm{ref}}^{\mathrm{r(i)}} \end{aligned} \tag{32}$$

with i as the index of each measured and analysed sample from the burst of N samples, $r(i)$ as the corresponding reference symbol, and t as the acquisition time relative to the symbol slot [13].

The definition of the reference vectors is the same as stated in 4.1. The normalization of the measured data follows the procedure outlined in 4.2 with the exception that only samples originating close to the centre of the symbol, e.g. some per cent of the symbol slot, are taken into account when determining the normalization factor α. When α is determined, the scaling applies to all samples in the measurement.

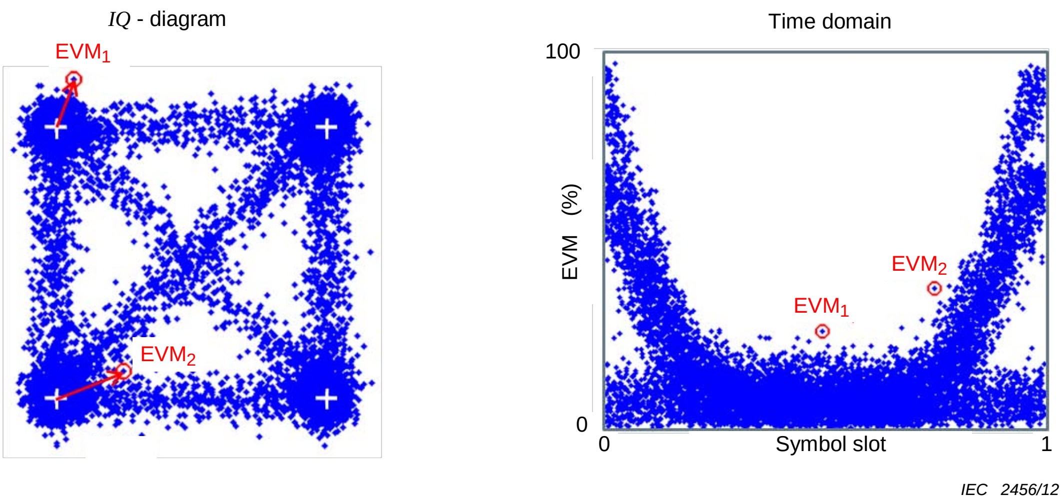

Figure 15 – *IQ*-diagram with indicated reference constellation and exemplary error vectors (left) and time domain plot of the EVM values for each measured sample (right)

The IQ-diagram in Figure 15 (left) shows all N samples in a burst with their associated amplitude and phase. The four white crosses indicate the reference vectors representing the ideal QPSK constellation normalized such that the EVM_{rms} is minimized. Two exemplary error vectors are indicated in red extending from the reference symbols to the associated measured samples. For each sample, an EVM value can be calculated in relation to its reference symbol. By implementing a time stamping mechanism in the test procedure, each sample can be coupled to its measurement time relative to the symbol slot. Figure 15 (right) shows the EVM value of each sample against their measurement time relative to the symbol slot. In the transition regions, the EVM values increase as the samples moves away from the ideal constellation.

A majority of the signal distortions that may influence the quality of vector modulated optical signals will strongly affect the transition region of the signals and hence change the appearance of the time-resolved EVM plot. Modulation distortions will show in the time-resolved EVM plot by both increasing the EVM in the symbol centres (higher EVM_{rms}) as well as reducing the opening in the time domain. The time-resolved EVM plot will give additional information compared to EVM_{rms} by better indicating margins to test failure and revealing reasons for test failures. There is a clear parallel to conventional mask testing, where an intensity mask is defined for a specific modulation format, and areas of the eye-diagrams are defined in which samples are forbidden to fall in order to pass the compliance test. With a similar approach, the time-resolved EVM plot is suitable for extension to time-resolved EVM mask testing. An exemplary mask is illustrated in the two plots of Figure 16. Note that the design of proper compliance test masks for different vector modulated optical signals is beyond the scope of this technical report. The two plots illustrate the two alternative referencing approaches: reference to nearest constellation point (left) or reference to the known correct constellation point (right). An exemplary mask is shown for illustrative purposes.

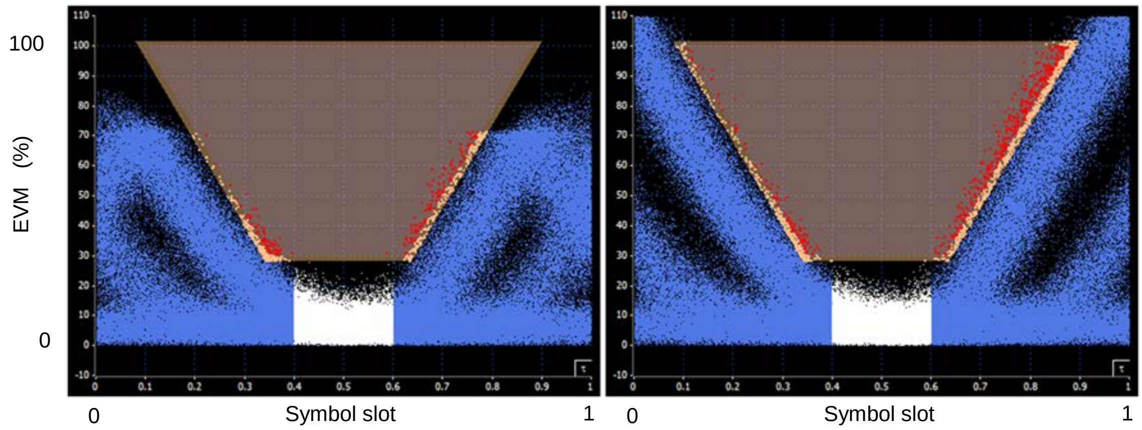

Figure 16 – Measured time-resolved EVM plots of a 28 GBd QPSK signal affected by 8 ps skew

Figure 17 shows two examples of measured time-resolved EVM of a 28 GBd QPSK signal which is distorted by 8 ps skew between the I and Q data signals. On the left, each sample is referenced to its nearest constellation point, and hence the EVM values are bounded by the extent of the decision quadrants of the QPSK signal. On the right, a signal with known symbol pattern was analysed and therefore the EVM can be related to the correct symbol for each symbol slot. In this case, the EVM can exceed 100 %. For most scenarios, both representations are accurate and will yield the same conclusions about the signal. For EVM noise characteristics, it is preferable to refer each sample back to the true symbol to avoid folding of the EVM values as the noise extends to neighbouring signal decision areas, e.g. when a symbol error occurs.

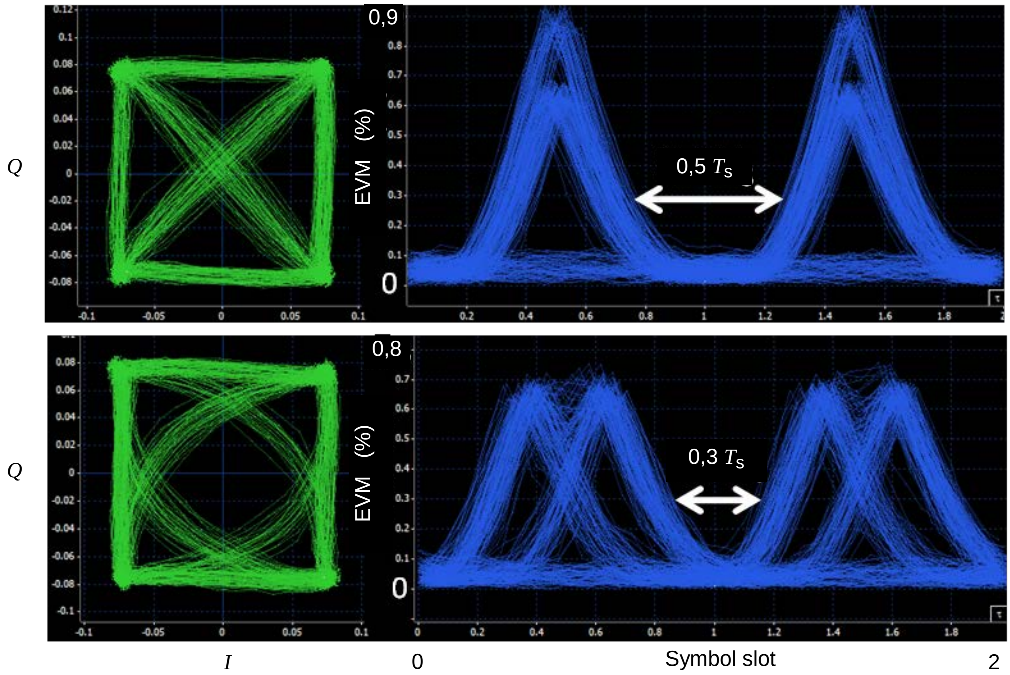

IEC 2458/12

Figure 17 – Noise-averaged *IQ*-diagrams and time-resolved EVM plots of a 28 GBd QPSK signal with 0 p skew (top) and 8 ps skew (bottom)

The time-resolved EVM concept can also be extended to include noise averaging of the EVM waveform. For signals with repetitive symbol pattern behaviour, it is possible to compute the EVM vs. time relative to the symbol pattern. In this case, noise averaging or noise filtering can be applied to the EVM symbol pattern to remove the impact of nondeterministic effects on the signal. The averaged time-resolved EVM symbol pattern can then be folded to averaged time-resolved EVM eye-diagram where every symbol is represented in a single symbol slot. Figure 17 shows the noise-averaged IQ-diagram (left) and noise-averaged time-resolved EVM plot (right) of a 28 GBd QPSK with 0 ps skew (top) and 8 ps skew (bottom). The noise averaging will enable more detailed analysis of the deterministic modulation impairments that may occur in a vector modulated optical signal transmitter. When compliance testing a vector modulated optical signal transmitter, the deterministic effects are of higher interest than the noise, and hence testing in a noise-free environment would be attractive. Compliance testing using masks could be adapted also to the noise-averaged time-resolved EVM environment with the advantage of enabling repeatable deterministic performance.

6.2 EVM with reference filter

The EVM reference, as described so far, either does not define the transition between symbols or implies steep transitions, implying unlimited bandwidth. Excessively steep transitions however correspond to increased spectral width for the signals, defeating the efficiency gains from vector modulation. In order to define the optimal transitions, a reference filter (raised cosine, root-raised cosine, etc.) can be applied to the sequence of detected symbols. An error vector for each consecutive measured sample with respect to the filtered reference can be displayed either as a consecutive series of error vectors or in the same way as time-resolved EVM. This compares the measured signal vectors against reference vectors representing a chosen optimum transition rather than an unrealistically steep transition.

The following set of images shows the influence of comparing the EVM of measured data against a reference signal with steep transition and raised-cosine filtered signal.

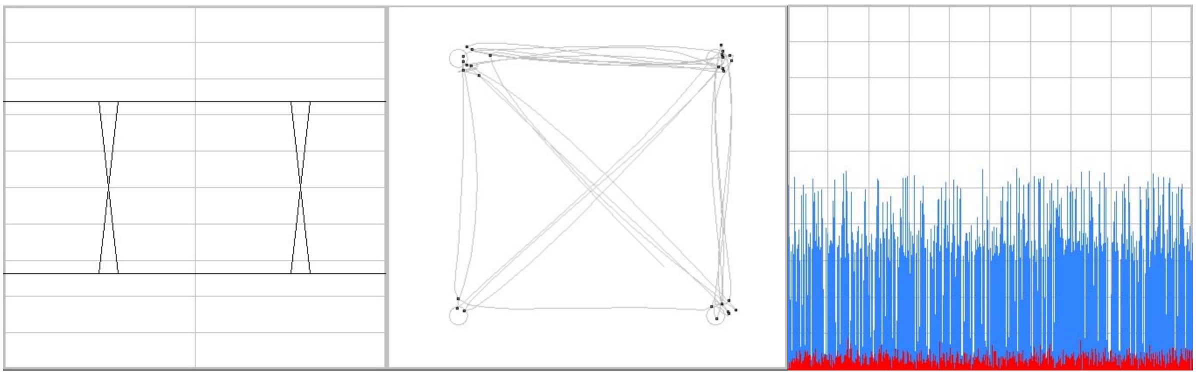

IEC 2459/12

Figure 18 – Eye-diagram of reference with steep transitions; measured signal *I-Q* diagram with symbols at decision time; EVM at symbol decision time (red) and EVM for all sample points (blue)

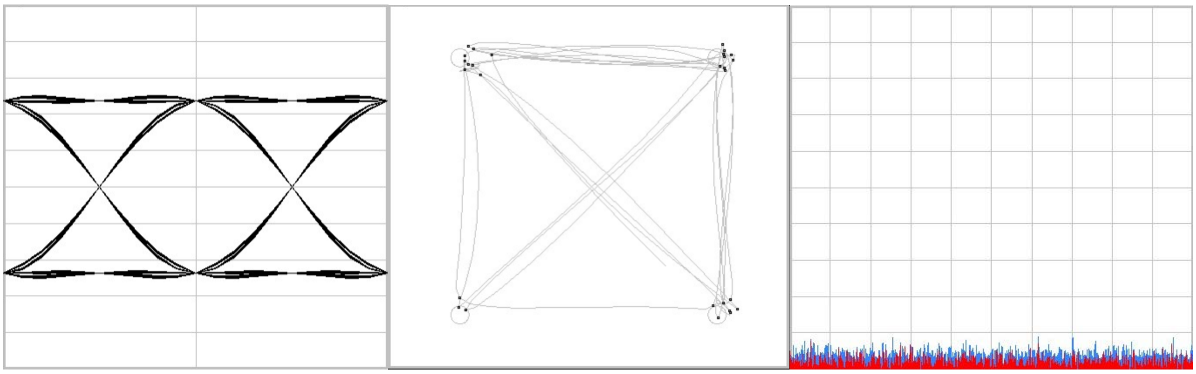

IEC 2460/12

Figure 19 – Eye-diagram of reference with raised-cosine filtering; measured signal *I-Q* diagram with symbols at decision time; EVM at symbol decision time (red) and EVM for all sample points (blue)

As can easily be seen from the two *I-Q* diagrams, the position of the symbols in the *I-Q* diagram is identical for raised-cosine filtering. This is not necessarily the case for all types of filters. However, the EVM at each sample point changes significantly between steep transition and raised-cosine-filtered references. Therefore, such a filtered reference can be used to evaluate how well signal transitions follow the desired trajectory.

6.3 Magnitude error

From the above-derived values in 4.2, the r.m.s. magnitude error expressed in % r.m.s. is calculated with the following equation. The formula applies to x and y polarization planes with respective data independently.

$$\mathrm{EM}_{\mathrm{rms,x}} = \sqrt{\frac{1}{N}\sum\nolimits_{n=1}^{N}\left(\left|\mathbf{S}_{\mathrm{norm,x}}(n)\right| - \left|\mathbf{S}_{\mathrm{ref,x}}^{r(n)}\right|\right)^2}$$
$$\mathrm{EM}_{\mathrm{rms,y}} = \sqrt{\frac{1}{N}\sum\nolimits_{n=1}^{N}\left(\left|\mathbf{S}_{\mathrm{norm,y}}(n)\right| - \left|\mathbf{S}_{\mathrm{ref,y}}^{r(n)}\right|\right)^2} \qquad (33)$$

6.4 Phase error

The r.m.s. phase error describes the r.m.s. deviation of phase around the ideal reference vector. The formula applies separately to the x and y polarization planes with respective data.

$$\phi_{\text{err,rms},x} = \sqrt{\frac{1}{N}\sum_{n=1}^{N}\left(\arctan\left(\frac{I_{\text{norm},x}(n)}{Q_{\text{norm},x}(n)}\right) - \arctan\left(\frac{I_{\text{ref}}^{r(n)}}{Q_{\text{ref}}^{r(n)}}\right)\right)^2}$$
$$\phi_{\text{err,rms},y} = \sqrt{\frac{1}{N}\sum_{n=1}^{N}\left(\arctan\left(\frac{I_{\text{norm},y}(n)}{Q_{\text{norm},y}(n)}\right) - \arctan\left(\frac{I_{\text{ref}}^{r(n)}}{Q_{\text{ref}}^{r(n)}}\right)\right)^2} \tag{34}$$

6.5 *I*-*Q* gain imbalance

The gain imbalance describes the error between the I and Q part of the signal. The formula applies separately to x and y polarization plane with respective data.

$$GI_x = 20\log\sqrt{\frac{1}{N}\sum_{n=1}^{N}\left(\frac{I_{\text{norm},x}(n)}{I_{\text{ref}}^{r(n)}} \bigg/ \frac{Q_{\text{norm},x}(n)}{Q_{\text{ref}}^{r(n)}}\right)^2}$$
$$GI_y = 20\log\sqrt{\frac{1}{N}\sum_{n=1}^{N}\left(\frac{I_{\text{norm},y}(n)}{I_{\text{ref}}^{r(n)}} \bigg/ \frac{Q_{\text{norm},y}(n)}{Q_{\text{ref}}^{r(n)}}\right)^2} \tag{35}$$

6.6 *I*-*Q* offset

The IQ_{offset} of the signal indicates a DC offset in the origin in the constellation diagram. This is displayed without offset as it is already removed by the reference receiver.

This data can be extracted from the values calculated in Clause 4.

$$IQ_{\text{offset,x}} = 20\log\sqrt{\left(\frac{1}{N}\sum_{n=1}^{N} I_{\text{norm},x}(n)\right)^2 + \left(\frac{1}{N}\sum_{n=1}^{N} Q_{\text{norm},x}(n)\right)^2}$$
$$IQ_{\text{offset,y}} = 20\log\sqrt{\left(\frac{1}{N}\sum_{n=1}^{N} I_{\text{norm},y}(n)\right)^2 + \left(\frac{1}{N}\sum_{n=1}^{N} Q_{\text{norm},y}(n)\right)^2} \tag{36}$$

6.7 Quadrature error

Quadrature error is caused by the I and Q channels not being determined precisely at 90° from each other. The quadrature error is referenced to the average vector of the demodulated symbols

$$\mathbf{S}_{\text{avg,x}}^{\text{r}} = \begin{pmatrix} I_{\text{avg},x}^{r} \\ Q_{\text{avg},x}^{r} \end{pmatrix} = \begin{pmatrix} \frac{1}{N}\sum_{n=1}^{N} I_{\text{norm},x}(n) \\ \frac{1}{N}\sum_{n=1}^{N} I_{\text{norm},x}(n) \end{pmatrix}$$
$$\mathbf{S}_{\text{avg,y}}^{\text{r}} = \begin{pmatrix} I_{\text{avg},y}^{r} \\ Q_{\text{avg},y}^{r} \end{pmatrix} = \begin{pmatrix} \frac{1}{N}\sum_{n=1}^{N} I_{\text{norm},y}(n) \\ \frac{1}{N}\sum_{n=1}^{N} I_{\text{norm},y}(n) \end{pmatrix} \tag{37}$$

where r =1-4 (for(D)QPSK) refers to the related symbol of the normalized measured I and Q component.

Quadrature error can be calculated for any symbol.

$$
\begin{aligned}
\gamma_x &= \frac{\pi}{2} - \left| \arccos\left(\frac{1}{2} \cdot \frac{\left(\left[I^r_{\mathrm{avg},x} \right]^2 - I^2_{\mathrm{ref}} \right) + \left(\left[Q^r_{\mathrm{avg},x} \right]^2 - Q^2_{\mathrm{ref}} \right)}{2 I_{\mathrm{ref}} \cdot Q_{\mathrm{ref}}} \right) \right| \\
\gamma_y &= \frac{\pi}{2} - \left| \arccos\left(\frac{1}{2} \cdot \frac{\left(\left[I^r_{\mathrm{avg},y} \right]^2 - I^2_{\mathrm{ref}} \right) + \left(\left[Q^r_{\mathrm{avg},y} \right]^2 - Q^2_{\mathrm{ref}} \right)}{2 I_{\mathrm{ref}} \cdot Q_{\mathrm{ref}}} \right) \right|
\end{aligned}
\qquad (38)
$$

Annex A
(informative)

Relationship between EVM and Q factor

For two-level signals, the Q factor is defined in the following way in IEC 61280-2-8:

$$Q = \frac{|\mu_1 - \mu_2|}{\sigma_1 + \sigma_2} \tag{A.1}$$

where μ_1 are the mean values of the two levels, and σ_1 the standard deviations of them.

Using the above definition of Q factor and the definition of the EVM and assuming isotropic noise in the IQ plane the following relationship holds true for QPSK modulation, based on the normalized two-level I or Q-components: with $|\mu_1\text{-}\mu_2|=\sqrt{2}$ and $\sigma_1= \sigma_2=\text{EVM}_{\text{rms}}/\sqrt{2}$.

$$Q_{\text{QPSK}} = \frac{1}{\text{EVM}_{\text{rms}}} \tag{A.2}$$

Generalizing this for multilevel formats like m-QAM ($m=k^2$) leads to the following definition of Q-factor for k-level signals:

$$Q = \frac{1}{k-1} \sum_{i=1..k-1} \frac{|\mu_{\text{i}} - \mu_{\text{i+1}}|}{\sigma_{\text{i}} + \sigma_{\text{i+1}}} \tag{A.3}$$

Again, assuming isotropic noise in the IQ plane the following relationship between EVM and Q-factor holds true:

$$Q_{\text{m-QAM}} = \frac{1}{(\sqrt{m} - 1) \times \text{EVM}_{\text{rms}}} \tag{A.4}$$

Annex B
(informative)

Details and implementations of vector signal measurement

The methods for measuring vector modulated optical signals are summarized in Table B.1.

Table B.1 – Methods for measuring vector modulated optical signals

	Real-time sampling (5.2.1)	Optical equivalent-time sampling (5.2.1)	One-symbol delayed interferometer (5.2.3)
Local oscillator	CW laser	Pulsed laser	Not used
Measured parameters	Amplitude and phase	Amplitude and phase	Phase
Bandwidth limitation	Electronics (several tens GHz)	Sampling pulse width (hundreds GHz)	Electronics (several tens GHz)
Sensitivity limitation	Shot noise	Shot noise	Thermal noise of electronics
Suitability for polarization multiplexed signals	Yes (with suitable post-processing)	Yes (with suitable post-processing)	Difficult

Bibliography

[1] MCKINLEY, Michael D., REMLEY, Kate A., MYSLINSKI, Maciej, STEVENSON KENNEY, J., SCHREURS, Dominique, NAUWELAERS, Bart, "*EVM Calculation for Broadband Modulated Signals*", 64th ARFTG Conf. Dig., Orlando, FL, pp. 45-52, Dec. 2004.

[2] IEEE Std 802.16™-2004 Revision of IEEE Std 802.16-2001.

[3] HASSUN, Roland, FLAHERTY, Michael, MATRECI, Robert, TAYLOR, Mitch "*Efffective Evaluation of Link Quality Using Error Vector Magnitude Techniques*", 1997 Wireless Communications Conference.

[4] SCHMOGROW, R., NEBENDAHL, B., WINTER, M., JOSTEN, A., HILLERKUSS, D. KOENIG, S., MEYER, J., DRESCHMANN, M., HUEBNER, M., KOOS, C., BECKER, J., FREUDE, W. and LEUTHOLD, J., "*Error Vector Magnitude as a Performance Measure for Advanced Modulation Formats*", IEEE Photon. Technol. Lett. 24, 61-63, 2012.

[5] KIKUCHI, K., "*Phase-diversity homodyne detection of multilevel optical modulation with digital carrier phase estimation*," IEEE. J. Sel. Top. Quantum Electron. Vol. 11, pp. 563-570, 2006.

[6] DORRER C. et al., "*Direct measurement of constellation diagrams of optical sources*," in Proc. Conf. Optical Fiber Communication, 2004, Paper PDP33.

[7] OKAMOTO K. et al., "*Ultrafast measurement of optical DPSK signals using 1-symbol delayed dual-channel linear optical sampling*," IEEE Photon. Tech. Lett. Vol. 20, No. 11, pp. 948-950, 2008.

[8] WILLIAMS, P.A., et al. "*Vector Signal Characterization of High-Speed Optical Components by Use of Linear Optical Sampling With Milliradian Resolution*," IEEE Photon. Tech. Lett. Vol. 20, No. 23, pp. 2007-2009, 2008.

[9] WESTLUND, M., SKOLD, M. and ANDREKSON, P., "*All-optical phase-sensitive waveform sampling at 40 GSymbol/s*" in Proceeding of Optical Fiber Conference 2008 (OFC 2008), PDP12.

[10] TANIMURA, K. and OHTA, H., "*Measurement of phase-distribution of phase-modulated optical signals using delayed self-homodyne detection*," ECOC 2006.

[11] TANIMURA, K. and OHTA, H., "*Monitoring of DPSK/DQPSK signals using 1-Bit delayed self-homodyne detection with optical phase diversity*" ECOC 2007.

[12] SAVORY, S.J., "*Digital Coherent Optical Receivers: Algorithms and Subsystems*", IEEE J. Sel. Topics Quantum Electron. 16, no. 5, pp. 1164–1179, 2010.

[13] SUNNERUD, H., WESTLUND, M., SKÖLD, M. and ANDREKSON, P., "*Time-Resolved Error Vector Magnitude for Transmitter Mask Testing in Coherent Optical Transmission Systems*", OFC/NFOEC 2011 (Los Angeles), Paper JWA031.

INTERNATIONAL
ELECTROTECHNICAL
COMMISSION

3, rue de Varembé
PO Box 131
CH-1211 Geneva 20
Switzerland

Tel: + 41 22 919 02 11
Fax: + 41 22 919 03 00
info@iec.ch
www.iec.ch